Andean Geology 48 (3): 546-556. September, 2021
doi: 10.5027/andgeoV48n3-3362

Andean Geology
www.andeangeology.cl

Local Cuban bentonite clay: composition, structure and textural characterization

***Pedro C. Quero-Jiménez[1, 2, 3], Lester A. Arias Felipe[3], Julio O. Prieto García[2], María E. Jorge Rodríguez[4], Jorge de la Torre[3], Osvaldo N. Montenegro[2], Reinaldo Molina-Ruiz[2], Inés S. Tiscornia[1]**

[1] *Institute of Catalysis and Petrochemical Research, National University of the Littoral, Argentina. S3000AOM Santa Fe, Argentina. pquero.jimenez@gmail.com; itiscornia@fiq.unl.edu.ar*

[2] *Centro de Bioactivos Químicos, Universidad Central "Marta Abreu" de Las Villas. Street to Camajuaní km 5 ½ Santa Clara. CP 54830, Villa Clara, Cuba. omarpg@uclv.edu.cu; onorman@uclv.edu.cu; reymolina@uclv.edu.cu*

[3] *Departamento de Licenciatura en Química, Universidad Central "Marta Abreu" de Las Villas. Street to Camajuaní km 5 ½ Santa Clara. CP 54830, Villa Clara, Cuba. laafe96@gmail.com; jbtl@uclv.edu.cu*

[4] *Departamento de Licenciatura en Farmacia, Universidad Central "Marta Abreu" de Las Villas. Street to Camajuaní km 5 ½ Santa Clara. CP 54830, Villa Clara, Cuba. elisa@uclv.edu.cu*

** Corresponding author: pquero.jimenez@gmail.com*

ABSTRACT. The physic and chemical characterization of the bentonite clay from the Chiqui Gómez deposit, central Cuba, (Cuban bentonite clay) shows that it is mainly constituted by sodium montmorillonite (>90%), with a structural formula for one-layer unit determined as $(Na_{3.99}Al_{0.01})(Al_{1.11}Fe^{3+}_{0.49}Mg_{0.18}Ti_{0.07})(Ca_{0.24}Na_{0.15}K_{0.01})O_{10}(OH)_2$. The Cuban bentonite clay has a specific surface area of 80 m^2g^{-1}, a pore volume of about 0.0776 cm^3g^{-1}, 61% porosity and both N_2 adsorption-desorption isotherms exhibit a hysteresis loop of IV type. The thermogravimetric analysis (TGA) of the studied mineral presents the first endothermic peak, characteristic of montmorillonite, in 48.1 ºC and others less accentuated (80.8, 94.0, 119.8 ºC) characteristic of sodium montmorillonite, that corresponds to the loss of water, and can be extended up to 250 ºC. The FT-IR spectra show the existence of Si-OH, Al-Al-OH, Al-Fe-OH, Al-Mg-OH and Si-O-Si functional groups in all clay samples, bands between 1,120 and 461 cm^{-1} correspond to phyllosilicate structures and OH stretching vibrations were observed. pH at the point of zero charge (pH_{PZC}) obtained has a value of 8.1, which allows montmorillonite to be classified as basic.

Keywords: Cuban bentonite clays, Montmorillonite, Characterization.

RESUMEN. Arcilla bentonítica cubana: composición, estructura y caracterización textural. La caracterización física y química de la arcilla bentonítica del depósito Chiqui Gómez, en el centro de Cuba, muestra que está constituida mayoritariamente (>90%) por montmorillonita sódica, con una fórmula estructural para una capa unitaria establecida como $(Na_{3,99}Al_{0,01})(Al_{1,11}Fe^{3+}_{0,49}Mg_{0,18}Ti_{0,07})(Ca_{0,24}Na_{0,15}K_{0,01})O_{10}(OH)_2$. Las arcillas de bentonita cubana tienen una superficie específica de 80 m^2g^{-1}, un volumen de poro de aproximadamente 0,0776 cm^3g^{-1} y una porosidad de 61%. Ambas isotermas de adsorción-desorción de N_2 exhibieron una isoterma de histéresis de tipo IV. El análisis termogravimétrico (TGA) del mineral estudiado presenta el primer pico endotérmico, característico de la montmorillonita, en 48,1 ºC y otros menos acentuados (80,8, 94,0, 119,8 ºC) característicos de la montmorillonita sódica, que corresponde a la pérdida de agua, y se puede extender hasta 250 ºC. Los espectros FT-IR mostraron la existencia de grupos funcionales Si-OH, Al-Al-OH, Al-Fe-OH, Al-Mg-OH y Si-O-Si en todas las muestras de arcilla, las bandas entre 1.120 y 461 cm^{-1} corresponden a estructuras de filosilicatos y se observaron vibraciones de estiramiento OH. El pH en el punto de carga cero (pH_{PZC}) obtenido tiene un valor de 8,1, lo que permite clasificar la montmorillonita como básica.

Palabras clave: Arcilla de bentonita cubana, Montmorillonita, Caracterización.

1. Introduction

Bentonite clays are widely distributed in the world (Grim and Güven, 1978). They are ores with montmorillonite as the main component and besides montmorillonite; bentonite contains other minerals, such as quartz, calcite, feldspar, muscovite and biotite (Petrović *et al.*, 2014). This mineral has properties such as charge density, surface charges, surface area, the type of exchangeable cations, silanol groups of crystalline defects or broken surfaces, hydroxyl groups on the edges, and Lewis and Bronsted acidity (Djomgoue and Njopwouo, 2013) which make it have a great adsorption capacity, this is why this mineral has multiple uses in different industrial processes.

The adsorption characteristics of bentonite depend on its chemical and mineralogical composition as well as on textural, structural and morphological characteristics (Petrović *et al.*, 2014). The use of bentonite as an adsorbent for oil impurities has been widely used and discussed in various investigations (Larouci *et al.*, 2015). Although bentonite can be used as an adsorbent in its natural form, some researchers have proposed experimental designs and methodologies for the acid activation of these minerals in order to optimize the purification process (Didi *et al.*, 2009; Palanisamy *et al.*, 2011; Ajemba, 2012; Usman *et al.*, 2013; Larouci *et al.*, 2015); when applying this activation method it should be borne in mind that excessive activation can be explained in terms of a loss of porosity and acid strength (Makhoukhi *et al.*, 2009). Also, acid treatment of bentonites has been shown to create mesoporosity depending on the acid concentrations and time of treatment involving major structural changes and partial decomposition of montmorillonite (Zheng *et al.*, 2017).

Nadhiro *et al.* (2018) studied the quality of *Sardinella lemuru* oil using bentonite as an adsorbent, revealing that the addition of activated bentonite can increase the quality of this oil that is canned in industry; meanwhile Suseno *et al.* (2014) showed in his research that the combination of different concentrations of natural bentonite followed by centrifugation is an excellent technique for purifying this oil, where the oil bleaching process tends to decrease as the concentration of the adsorbent is decreased and centrifugation speed. The aim of the present study is to characterize the bentonite clays of the Chiqui Gómez bentonite deposit in Cuba (denominated as Cuban bentonite clays in this work) due to the potential of this unexploited deposit, which could be used as adsorbent of shark liver oil impurities. To this end, their mineralogy, chemistry, textural, structural and morphological characteristics were determined.

2. Materials and methods

2.1. Materials

The raw clay samples (Fig. 1) used in the present work were collected from the deposit Bentonita Chiqui Gómez (X=633,200; Y=311,350) which is located in Remedio, 44 km northeast Villa Clara in the Central Region of Cuba. The samples were provided by Empresa Geominera del Centro, which has a processing capacity of 2 Kt/year. They contain 50-60% mixed-layered illite-smectite (I-S) with 80-85% expandable layers, minor clinoptilolite, quartz, opal-CT, carbonates (calcite and trace siderite) and trace of gypsum and kaolinite.

The Bentonita Chiqui Gómez deposit or concession, is part of the Camacho Formation lithostratigraphic unit; which is an Upper Pleistocene sedimentary deposit. This is made up of sandy-clayey silts and silty clays with a grayish brown color, with intercalations of fine gravels and carbonates concretions, as well as dispersed gypsum crystals. The bentonite bearing layer can reach a thickness of up to 3 m and is distributed in the provinces of Sancti Spíritus and Villa Clara in the center of Cuba.

FIG. 1. Natural bentonite used in this study.

2.2. Sample preparation

All bentonite samples (10) were dried at 105 ℃ for 4 h in a drying air oven and then were grounded using a porcelain mill to pass through a mesh size screen of 50 μm. A composite sample was formed by the combination of 10 primary samples, taking into account that samples are truly representative of the deposit. This sample was ready for chemical analysis and physical-chemical tests including the DRX analysis.

2.3. Physicochemical characterizations of the Cuban bentonite clays

The physical characterization of the bentonite is carried out from the density determination: pycnometric with glass pycnometer, apparent and apparent by imprisonment (Kaufhold *et al.*, 2012); porosity (Tadros, 1980; Krupskaya *et al.*, 2019), flow rate (Elo *et al.*, 2019); compressibility (Kahr and Madsen, 1995) and tortuousness. The chemical composition of the bentonite samples was performed by atomic absorption spectroscopy (CBG 933 AA, Melbourne, Australia). This analysis of chemical composition was corroborating by Energy Dispersive Spectrometry (EDS).

2.3.1. Textural properties

The textural properties of the bentonite samples were determined with a Micromeritics ASAP 2020 analyzer. 0.1001 g of raw bentonite were previously degassed at 170-200 °C for 8 h. The total pore volume was measured at a relative pressure (P/P_o) from 0 to 0.99. Adsorption isotherms were determined by N_2 adsorption over the samples at -196 ºC. The Brunauer-Emmet-Teller (BET) and Barrette-Joynere-Halenda (BJH) equations were used to calculate the specific surface area and average pore diameter of the materials from nitrogen adsorption and desorption isotherms.

2.3.2. Scanning Electron Microscopy (SEM) and Energy Dispersive Spectrometry (EDS)

With the objective of studying their morphology, bentonite natural powder sample were examined with a scanning electron microscope PhenomProX (SEM, operated at 15 kV). The elemental chemical analysis in the film was performed using a fully integrated EDS detector and software of the mentioned microscope.

2.3.3. X-ray diffraction (XRD) characterization

X-Ray diffraction peaks of bentonite clay samples were measured on a Shimadzu XD-D1 diffractometer with monochromator using a Cu-Kα radiation at a scanning rate of 2º min^{-1} in 2θ=10-70º. The peaks observed for the catalysts were compared to standards published by JCPDS data (Joint Committee on Powder Diffraction Standards). The crystallites size was estimated by Scherrer's equation. The 2D ordered layers structure of material was verified by low angle X-ray diffraction. The patterns were recorded on a Panalytical, X'PertCelerator (50 kV voltage), using a Cu-Kα (λ=1.54183 Å) as the X-ray source. The signal was recorded for 2θ=5 to 60º with a step of 0.5º s^{-1}. The d-spacing (100) and the unit-cell parameter a_0 were calculated from the basic equation of the Bragg law (λ/2=sen θ and $2.d_{100}/\sqrt{3}$ respectively).

2.3.4. Thermal analysis

The thermal behavior of the bentonite clays was studied in a Mettler Toledo TGA/SDTA 851 instrument. The weight changes and the differential thermal process of the material (10 mg of samples) were analyzed from 25 up to 1,000 °C with a heating rate of 10 °C min^{-1} in air flow (80 ml min^{-1}).

2.3.5. Fourier transform infrared (FT-IR) spectrophotometry

FT-IR Spectrophotometer Shimadzu IR Prestige 21™ (Germany) was used to analyze bentonite clay samples. Spectra ranges were set at 4,000 to 400 cm^{-1}, using the IRsolution Agent software. The resulting spectra were directly compared with the reference library databases.

2.3.6. Determination of point of zero charge and Boehm titration

The acidity and total basicity of the bentonite is determined using the Boehm method (Boehm, 1966, 2002; Rezma *et al.*, 2019). pH_{pzc} is the pH at which the net particle charge becomes zero, it is an important parameter for describing surface behavior. Initial pH values (pH_i) of 20 mL of KCl solutions (concentrations 10^{-3} and 10^{-2} mol L^{-1}) were adjusted in pH range of 3.1 to 10 using 0.01 mol L^{-1} of HCl or NaOH. Then, 0.05 g of Cuban bentonite clays was added to each sample. Equilibration was carried out by shaking, in a rotary incubator at 200 rpm for 2h at 25±1 ºC. The dispersions were then

filtered and the final pH of the solutions (pH_f) was determined, point of zero charge was found from a plot of pH_f versus pH_i.

2.4. Statistical analysis

Results were expressed as mean values ± standard deviation (SD) (n=3). The R statistical software package (version 3.6.3) and Stat Graphics Centurion XV (version 15.2.06) was used to generate the orthogonal matrix of the design, response surface methodology modeling, statistical analysis, and regression models.

3. Results and discussion

3.1. Characterization of the Cuban bentonite clays

The results obtained in the physical characterization are presented in table 1.The studied material presents a pycnometric density in the range reported by Quintana (2013) for cuban bentonite clay; likewise the apparent density by trapping indicates that it can be compressed practically by 50%. Bentonite clays studied presents a relatively high porosity value, above 50%, a manifestation of its high roughness and capillary action. The compressibility demonstrates the high degree of compaction, as it reduces its original volume to almost a quarter. The tortuousness values reflect a high degree of disorder of the channels and surface of the solid. The value of the flow velocity obtained (V_f equal to zero) corroborates the relative high value of porosity.

The N_2 adsorption-desorption isotherms of the Cuban bentonite clay (Fig. 2) exhibit a hysteresis loop of IV type (Zhang *et al.*, 2016). Such hysteresis loops are related to slit-shaped pores or ink-bottle pores (Fig. 2). The specific surface area of the Cuban bentonite clay (80 m^2g^{-1}) is in the lower range of the values reported by Hevia (2007) and Romero and Barrios (2006)[1]. Compared to the values reported by Hernández *et al.* (2003) for partially destroyed montmorillonite and quartz (325 m^2g^{-1}) and, montmorillonite and quartz (303 m^2g^{-1}) from Tehuacán, Puebla in Mexico this value is considered relatively low. However, it is slightly lower than the value reported by León Barrios and Díaz Díaz (2019) for a Na bentonite from the Manuagua deposit in La Habana province, Cuba (102 m^2g^{-1}). Aditionally, the natural bentonite from Santa Catarina State, in Brazil studied by Foletto *et al*. (2013) displays a specific surface area of 16.45 m^2g^{-1}, substantially lower than the result obtained for the bentonite considered in this study, so the value obtained in our research would be high, a similar result is also observed in raw bentonite from Hammam Boughrara (Maghnia, Algeria) that shows a specific surface area of 29.23 m^2g^{-1} (Korichi *et al*., 2009). Pore volume was 0.0776 cm^3g^{-1} for Cuban bentonite clay.

The X-ray diffractogram of raw bentonite shows that the main mineralogical component is montmorillonite (>90%) together with minor amounts of plagioclase, cristobalite, calcite and almost undetectable presence of quartz (Fig. 3). XRD peaks are assigned according to the literature (Chihi *et al.*, 2019; Gan *et al.*, 2019). This analysis allows verifying the presence of dioctahedral smectite (spaced d: 14.65 Å, 4.39 Å, 4.13 Å and 2.53 Å) as the main component, and feldspar (d: 3.08 Å) correspondent to albite-anortite series (Ab-30% and An-70%) as minor phase. The diffraction signal d_{060} makes it possible to distinguish between di-octahedral and tri-octahedral smectites, because the dimension of the cell on the b axis is sensitive to the size of the cations and the occupation of the sites in the octahedral layer (Moore and Reynolds, 1997; Zhou *et al.*, 2018). The value of d_{060}=1.50 Å is typical and confirms the di-octahedral character, deduced from the structural formula, and from the information obtained by chemical analysis, where the Si/Al ratio indicated a characteristic value for this type of smectites.

The thermogravimetric analyses (TGA) verify the presence of the montmorillonite in the sample under study. The analyzed sample presents the first endothermic peak, characteristic of montmorillonite, at 48.1 ºC and others less accentuated (80.8, 94.0, 119.8 ºC) characteristic of sodium montmorillonite, that correspond to the loss

TABLE 1. PHYSICAL PROPERTIES OF THE CUBAN BENTONITE CLAY.

Physical parameters	Experimental values	Standard deviation (n=3)
Pycnometric density	2.09 g/mL	0.015
Apparent density	0.81 g/mL	0.027
Granular density	1.15 g/mL	0.004
Porosity	61.00 %	0.000
Compressibility	29-83 %	0.000
Tortuousness	1.19 g/mL	0.004

[1] Romero, E.G.; Barrios, M.S. 2006. Las arcillas: propiedades y usos. Available at: http://campus.usal.es/~delcien/doc/GA.PDF (last visited 11-08-2020).

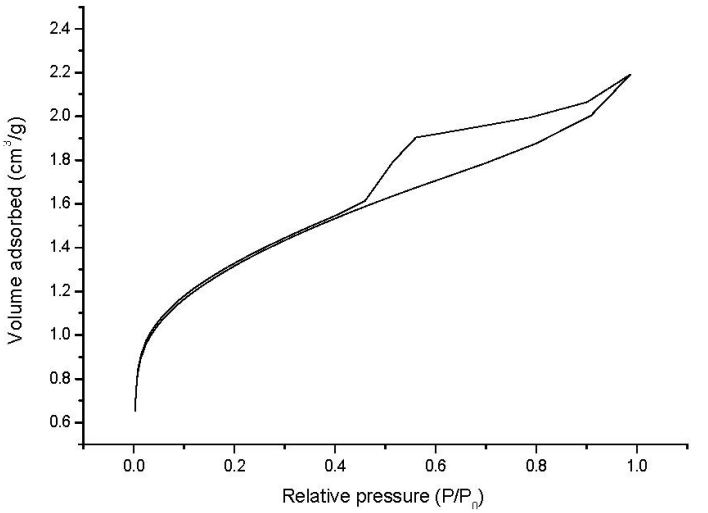

FIG. 2. N_2 adsorption isotherms of the Cuban bentonite clay.

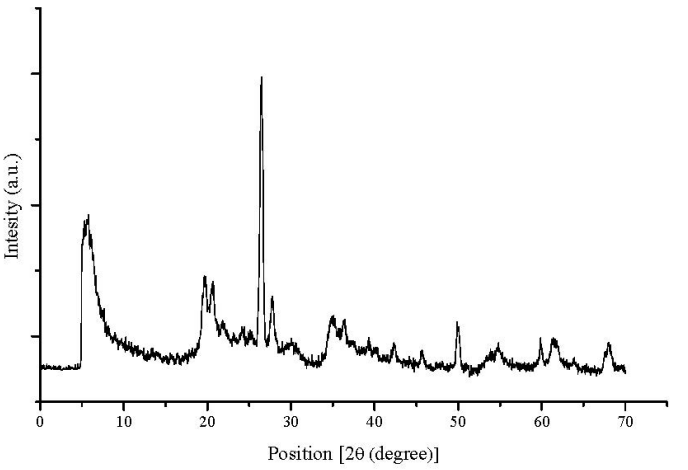

FIG. 3. XRD diffractogram of Cuban bentonite clay (mineralogical identification).

of water, and can be extended up to 250 ºC. The small peak at 406.7 ºC represents the loss of water from the montmorillonite hydroxyl, specifically from calcium. So at 579.7 ºC, a small endothermic reaction can be observed, which may indicate the initial stage of transformation of montmorillonite, decomposition or phase change of an impurity. The weight loss was around 9.5%, which means the percentage of water in the sample and is less than the content reported, for example, by Neira *et al.* (2007) for Colombian bentonite.

The FT-IR spectrum of Cuban bentonite clay (Fig. 4) reveals the bands belonging to montmorillonite: those assigned to Si-O in-plane and out-of-plane stretching vibrations at 1,050 to 1,118 cm^{-1}, respectively, as well as the ones corresponding to bending vibrations of Al-Al-OH, Al-Fe-OH and Al-Mg-OH at 917, 875, 840 cm^{-1}, respectively (Kaufhold *et al.*, 2002; Madejová, 2003; Gereli *et al.*, 2006; Klinkenberg *et al.*, 2006; Madejová *et al.*, 2006; Tyagi *et al.*, 2006; Scholtzová *et al.*, 2014). The spectrum obtained has the characteristic

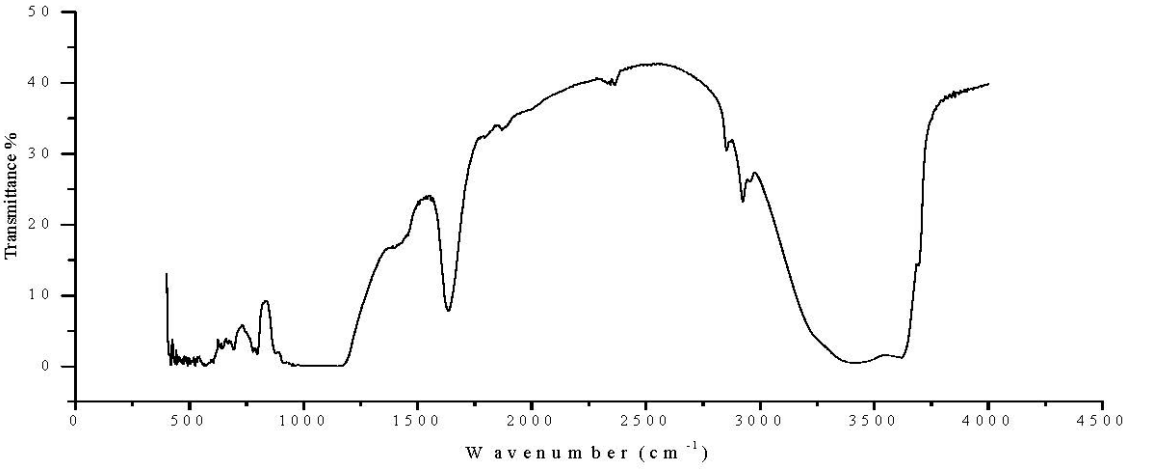

FIG. 4. FT-IR spectrum of Cuban bentonite clay.

appearance of clay minerals and in particular of smectites. The bands between 1,120 and 461 cm^{-1} correspond to phyllosilicate structures. Three well differentiated regions are observed. In the area with the highest wave numbers (3,600 to 3,400 cm^{-1}) OH stretching vibrations are identified, that can arise from the isomorphic substitution in the tetra and octahedral layers in bentonite (Wilson, 1994), occasionally in 3,424 cm^{-1} a slightly wide band is observed denoting the presence of water absorbed or united by elements Al and Mg (Chukanov and Chervonnyi, 2016). The area with the lowest wave values (518-461 cm^{-1}) indicates the characteristic stretch vibrations of Si-O (518 cm^{-1}) and deformation Si-O-Si (461 cm^{-1}). The aluminum character of the octahedral layer is manifested by the intensity of the absorption band centered at 1,031 cm^{-1}, which is assigned to the deformation of Al-Al-OH bonds (Jafar *et al*., 2015).

The pH at the point of zero charge (pH_{PZC}) obtained has a value of 8.1, which allows montmorillonite to be classified as basic; this indicates the possibility of adsorbing metal ions and confirms the classification as sodium (Ijagbemi *et al*., 2009). Also important was the fast equilibration observed for successive increments of HCl during the titration process. This may suggest a relatively short time of adsorption, making negligible the effects of other processes such as dissolution that could affect proton adsorption especially at low pH (Duc *et al*., 2005). The fast equilibration, leading to rapid pH stability can be interpreted as a result of reactions between protons and hydroxylated surface sites which are known to be very fast reactions (Unger, 1979; Thissen, 2020). A similar behavior was observed during the acid-base potentiometric titrations with different KCl electrolyte concentrations to measure the proton adsorption (Ijagbemi *et al*., 2009).

3.2. Elemental analysis

The chemical composition of the analyzed samples is presented in table 2.

On the basis of the elemental analysis of the montmorillonite, obtained by the average of EDX

TABLE 2. CHEMICAL COMPOSITION OF THE CUBAN BENTONITE CLAY.

	Composition (wt%)	Standard deviation (n=3)
SiO_2	54.10	0.017
Al_2O_3	12.72	0.021
Fe_2O_3	8.70	0.008
TiO_2	0.94	0.021
CaO	3.05	0.023
MgO	1.67	0.011
Na_2O	1.06	0.009
K_2O	0.20	0.027
loss on ignition at 900 °C	17.56	0.005

chemical analysis (Fig. 5), the resulting structural formula is: $(Na_{3.99}Al_{0.01})(Al_{1.11}Fe^{3+}_{0.49}Mg_{0.18}Ti_{0.07})(Ca_{0.24}Na_{0.15}K_{0.01})O_{10}(OH)_2$ and indicate the location of the different cations in metal oxide octahedrons or tetrahedrons, respectively. Aluminum was assigned to tetrahedral positions to complete an occupancy of eight, then magnesium and iron were assigned to octahedral sites and completed an occupancy of four, sodium ions were assigned to the interlayer. The resulting formula represents a Wyoming-type montmorillonite (sodium montmorillonite), according to the classification by Schultz (1969), because of the layer charge, lower than 0.85 electron charges per unit cell (e^-/u.c.), and the percentage of tetrahedral substitution.

The bentonite under study is a montmorillonite with low isomorphic substitution in the tetrahedral layer. The number of atoms in the octahedral layer is very close to the theoretical value of 2.0 for a dioctahedral mineral and the number of interlamina cations (0.40) is also very close to the reported 0.33. The layer load is -0.57, a value that is in the range of -0.2 to -0.6 established as a classification criterion and the load balance is practically zero (0.07).

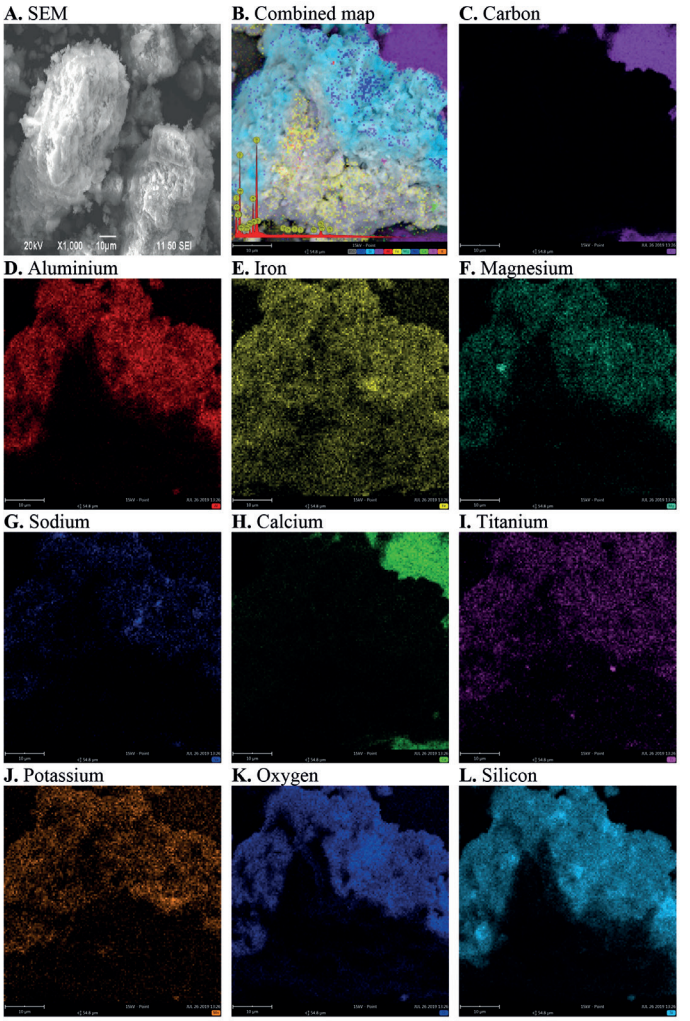

FIG. 5. **A.** SEM micrographs of the Cuban bentonite clays (magnification: x1000); **B.** Combined element mapping and EDX spectra for the raw bentonite; **C.** C-element mapping; **D.** Al-element mapping; **E.** Fe-element mapping; **F.** Mg-element mapping; **G.** Na-element mapping; **H.** Ca-element mapping; **I.** Ti-element mapping; **J.** K-element mapping; **K.** O-element mapping; **L.** Si-element mapping.

The dominant ion in the octahedron is aluminum, so it can be considered that it is an aluminum dioctahedral montmorillonite. The previous results are in line with those obtained by other authors (Jones and Handreck, 1967; Wazamtu *et al.*, 2013), in similar works, regarding the presence of high percentage values of silica, followed by alumina and iron oxide, the latter being influential in the coloration of the sample, the oxides of magnesium and calcium are higher than those of potassium and sodium. They also have lower percentages of titanium oxide, frequently found in clays (Chihi *et al.*, 2019; Deepracha *et al.*, 2019). The relationship between the Si/Al ratios obtained is 4.25, which is much higher than the range reported by Daza *et al.* (2004) and Enciso *et al.* (2005) for clay of the bentonite types in Colombia. The highest oxide percentages correspond to SiO_2 and Al_2O_3, which together with that of Fe_2O_3, correspond to those reported by Chihi *et al.* (2019). When comparing the chemical composition of the studied sample with that of sodium and calcium bentonite types (Abdullahi and Audu, 2017), some correspondence with both can be observed in terms of SiO_2 and Al_2O_3 contents. However, the Fe_2O_3 content is lower than that reported for the two previously mentioned bentonite types, but closer to those of calcium rich ones. Na_2O content is half of that reported for sodium rich bentonite, while the CaO content duplicates the reported values for the same type of bentonite, but in the range of those reported by Quintana (2013) for Cuban bentonites.

Scanning electron microscopy analyzes allowed determining the morphology of the starting mineral (Fig. 5). The micrograph of the bentonite under study allowed observing dispersed particles of different sizes, no larger than 10 µm. The lamellar aggregates joined by coalescence forming a flake-shaped structure can be seen in detail. The presence of rolled tubular laminar shapes confirms the dioctahedral character of the bentonite under study. From the results obtained by the different methods and the analysis of the calculated structural formula, it is concluded that the bentonite under study is mainly composed by sodium montmorillonite, with a specific surface area of 80 m^2g^{-1} and 61% of porosity.

Finally, the chemical composition and physical properties of the studied bentonite indicate that it is suitable for use in the purification of oils (Maskan and Bagci, 2003).

4. Conclusions

The physic and chemical characterization of the Cuban bentonite clays shows that it is mainly constituted by sodium montmorillonite (>90%), with a structural formula for one-layer unit determined as $(Na_{3.99}Al_{0.01})(Al_{1.11}Fe^{3+}_{0.49}Mg_{0.18}Ti_{0.07})(Ca_{0.24}Na_{0.15}K_{0.01})O_{10}(OH)_2$. The studied bentonite has a specific surface area of 80 m^2g^{-1}, a pore volume of about 0.0776 cm^3g^{-1}, 61% porosity and both N_2 adsorption-desorption isotherms exhibit a hysteresis loop of IV type. These characteristic indicate that Cuban bentonite is suitable for use in oil purification.

Acknowledgements

We gratefully acknowledge the Facultad de Ingeniería Química of the Universidad Nacional del Litoral (FIQ-UNL) and the Centro Nacional de Catálisis (CENACA) in Argentina for their technical support. The reviewers are also thanked for their always constructive comments during the review process.

Declaration of competing interest

No conflict of interest is declared.

References

Abdullahi, S.L.; Audu, A.A. 2017. Comparative analysis on chemical composition of bentonite clays obtained from Ashaka and Tango Deposits in Gombe State, Nigeria. ChemSearch Journal 8 (2): 35-40.

Ajemba, R.O. 2012. Optimum activation conditions of ughelli bentonite for palm oil bleaching using response surface methodology. Australian Journal of Basic and Applied Sciences 6 (12): 186-197.

Boehm, H. 1966. Chemical Identification of Surface Groups. *In* Advances in Catalysis (Eley, D.D.; Pines, H.; Weisz, P.B.; editors). Academic Press 16: 179-274. Cambridge. doi: 10.1016/S0360-0564(08)60354-5.

Boehm, H. 2002. Surface oxides on carbon and their analysis: a critical assessment. Carbon 40 (2): 145-149. doi: 10.1016/S0008-6223(01)00165-8.

Chihi, R.; Blidi, I.; Trabelsi-Ayadi, M.; Ayari, F. 2019. Elaboration and characterization of a low-cost porous ceramic support from natural Tunisian bentonite clay. Comptes Rendus Chimie 22 (2-3): 188-197. doi: 10.1016/j.crci.2018.12.002.

Chukanov, N.V.; Chervonnyi, A.D. 2016. Infrared Spectroscopy of Minerals and Related Compounds.

Springer International Publishing (Springer Mineralogy): 1109 p. Switzerland. doi: 10.1007/978-3-319-25349-7.

Daza, C.; Moreno, S.; Molina, R. 2004. Bentonita colombiana modificada con Al-Cu para la oxidación de fenol en medio acuoso diluido. Scientia Et Technica 10 (25): 265-270.

Deepracha, S.; Vibulyaseak, K.; Ogawa, M. 2019. Complexation of TiO_2 with clays and clay minerals for hierarchically designed functional hybrids. *In* Advanced Supramolecular Nanoarchitectonics (Ariga, K.; Aono, M.; editors). Elsevier: 125-150. doi: 10.1016/B978-0-12-813341-5.00010-3.

Didi, M.; Makhoukhi, B.; Azzouz, A.; Villemin, D. 2009. Colza oil bleaching through optimized acid activation of bentonite. A comparative study. Applied Clay Science 42 (3-4): 336-344. doi: 10.1016/j.clay.2008.03.014.

Djomgoue, P.; Njopwouo, D. 2013. FT-IR spectroscopy applied for surface clays characterization. Journal of Surface Engineered Materials and Advanced Technology 3 (4): 275-282. doi: 10.4236/jsemat.2013.34037.

Duc, M.; Gaboriaud, F.; Thomas, F. 2005. Sensitivity of the acid-base properties of clays to the methods of preparation and measurement. Journal of Colloid and Interface Science 289 (1): 139-147. doi: 10.1016/j.jcis.2005.03.060.

Elo, O.; Hölttä, P.; Kekäläinen, P.; Voutilainen, M.; Huittinen, N. 2019. Neptunium (V) transport in granitic rock: A laboratory scale study on the influence of bentonite colloids. Applied Geochemistry 103: 31-39. doi: 10.1016/j.apgeochem.2019.01.015.

Enciso, Y.H.; Moreno, S.; Molina, R. 2005. Modificación de bentonita con Al-Fe a partir de suspensiones concentradas de arcilla. Revista de Ingeniería e Investigación 57: 49-57.

Foletto, E.L.; Paz, D.S.; Gündel, A. 2013. Acid-activation assisted by microwave of a Brazilian bentonite and its activity in the bleaching of soybean oil. Applied Clay Science 83-84: 63-67. doi: 10.1016/j.clay.2013.08.017.

Gan, F.; Hang, X.; Huang, Q.; Deng, Y. 2019. Assessing and modifying China bentonites for aflatoxin adsorption. Applied Clay Science 168: 348-354. doi: 10.1016/j.clay.2018.12.001.

Gereli, G.; Seki, Y.; Kuşoğlu, I.M.; Yurdakoç, K. 2006. Equilibrium and kinetics for the sorption of promethazine hydrochloride onto K10 montmorillonite. Journal of Colloid and Interface Science 299 (1): 155-162. doi: 10.1016/j.jcis.2006.02.012.

Grim, R.E.; Güven, N. 1978. Geological features and mineralogical studies of major bentonite occurrences. *In* Bentonites; Geology, Mineralogy, Properties and Uses (Grim, R.E.; Güven, N.; editors). Elsiever: 13-160. doi: 10.1016/S0070-4571(08)70613-7.

Hernández, M.Á.; Velasco, J.A.; Rojas, F.; Lara, V.H.; Salgado, M.A.; Tamariz, V. 2003. Evaluación de mesoporos y caracterización de arcillas del estado de Puebla, México. Revista Internacional de Contaminación Ambiental 19 (4): 18-190.

Hevia, R. 2007. Bentonitas: Propiedades y usos industriales. Servicio Geológico Minero Argentino (Segemar), Céramica y Cristal 3: 49-52.

Ijagbemi, C.O.; Baek, M.H.; Kim, D.S. 2009. Montmorillonite surface properties and sorption characteristics for heavy metal removal from aqueous solutions. Journal of Hazardous Materials 166 (1): 538-546. doi: 10.1016/j.jhazmat.2008.11.085.

Jafar, B.M.; Hamadneh, I.; Khalili, F.I.; Al-Dujaili, A.H. 2015. Kinetic study on adsorption of fatty hydroxamicacids by natural clays. Jordan Journal of Earth and Environmental Sciences 7 (1): 11-17.

Jones, L.H.P.; Handreck, K.A. 1967. Silica In Soils, Plants, and Animals. Advances in Agronomy 19: 107-149. doi: 10.1016/S0065-2113(08)60734-8.

Kahr, G.; Madsen, F.T. 1995. Determination of the cation exchange capacity and the surface area of bentonite, illite and kaolinite by methylene blue adsorption. Applied Clay Science 9 (5): 327-336. doi: 10.1016/0169-1317(94)00028-O.

Kaufhold, S.; Dohrmann, R.; Ufer, K.; Meyer, F.M. 2002. Comparison of methods for the quantification of montmorillonite in bentonites. Applied Clay Science 22 (3): 145-151. doi: 10.1016/S0169-1317(02)00131-X.

Kaufhold, S.; Plötze, M.; Klinkenberg, M.; Dohrmann, R. 2012. Density and porosity of bentonites. Journal of Porous Materials 20: 191-208. doi: 10.1007/s10934-012-9589-7.

Klinkenberg, M.; Dohrmann, V.; Kaufhold, V.; Stanjek, H. 2006. A new method for identifying Wyoming bentonite by ATR-FTIR. Applied Clay Science 33 (3-4): 195-206. doi: 10.1016/j.clay.2006.05.003.

Korichi, S.; Elias, A.; Mefti, A. 2009. Characterization of smectite after acid activation with microwave irradiation. Applied Clay Science 42 (3-4): 432-438. doi: 10.1016/j.clay.2008.04.014.

Krupskaya, V.; Novikova, L.; Tyupina, E.; Belousov, P.; Dorzhieva, O.; Zakusin, S.; Kim, K.; Roessner, F.; Badetti, E.; Brunelli, A.; Belchinskaya, L. 2019. The influence of acid modification on the structure of montmorillonites and surface properties of bentonites. Applied Clay Science 172: 1-10. doi: 10.1016/j.clay.2019.02.001.

Larouci, M.; Safa, M.; Meddah, B.; Aoues, A.; Sonnet, P. 2015. Response surface modeling of acid activation of raw diatomite using in sunflower oil bleaching by: Box-Behnken experimental design. Journal of Food Science and Technology 52 (3): 1677-1683. doi: 10.1007/s13197-013-1113-9.

León Barrios, M.; Díaz Díaz, M.Á. 2019. Modificación de bentonita cubana y su aplicación como adsorbente de hidrocarburos. Tecnología Química 39 (3): 552-563.

Madejová, J. 2003. FTIR techniques in clay mineral studies. Vibrational Spectroscopy 31 (1): 1-10. doi: 10.1016/S0924-2031(02)00065-6.

Madejová, J.; Pálková, H.; Komadel, P. 2006. Behaviour of Li^{+} and Cu^{2+} in heated montmorillonite: Evidence from far-, mid-, and near-IR regions. Vibrational Spectroscopy 40 (1): 80-88. doi: 10.1016/j.vibspec.2005.07.004.

Makhoukhi, B.; Didi, M.A.; Villemin, D.; Azzouz, A. 2009. Acid activation of Bentonite for use as a vegetable oil bleaching agent. Grasas y Aceites 60 (4): 343-349. doi: 10.3989/gya.108408.

Maskan, M.; Bagci, H. 2003. Effect of different adsorbents on purification of used sunflower seed oil utilized for frying. European Food Research and Technology 217 (3): 215-218. doi: 10.1007/s00217-003-0731-2.

Moore, D.M.; Reynolds, R.C. 1997. X-Ray Diffraction and the Identification and Analysis of Clay Minerals. Clay Minerals 34 (1): 210-211. doi: 10.1180/claymin.1999.034.1.21.

Nadhiro, U.; Subekti, S.; Tjahjaningsih, W.; Patmawati, W. 2018. Quality characteristics of Bali sardinella (*Sardinella lemuru*) oil purified with bentonite as an adsorbent. IOP Conference Series: Earth and Environmental Science 137 (12012): 1-5. doi: 10.1088/1755-1315/137/1/012012.

Neira, G.; Barrera, M.; Mejía, I.; Palacios, J.F.; Henao, J.A. 2007. Preparación de nanocompuestos de polímero/silicato usando bentonitas colombianas modificadas. Scientia Et Technica (36): 591-595.

Palanisamy, U.D.; Sivanathan, M.; Radhakrishnan, A.K.; Haleagrahara, N.; Subramaniam, T.; Chiew, G.S. 2011. An effective ostrich oil bleaching technique using peroxide value as an indicator. Molecules 16 (7): 5709-5719. doi: 10.3390/molecules16075709.

Petrović, Z.; Dugić, P.; Aleksić, V.; Begić, S.; Sadadinović, J.; Mićić, V.; Kljajić, N. 2014. Composition, structure and textural characteristics of domestic acid activated bentonite. Contemporary Materials 1: 133-139.

Quintana, R. 2013. Adsorción de zinc mendiante bentonita. *In* Sociedad Cubana de Geología (editor) Geociencias, Ciencias de la Tierra al Servicio de la Sociedad: p. 2 La Habana.

Rezma, S.; Ben Assaker, I.; Litaiem, Y.; Chtourou, R.; Hafiane, A.; Deleuze, H. 2019. Microporous activated carbon electrode derived from date stone without use of binder for capacitive deionization application. Materials Research Bulletin 111: 222-229. doi: 10.1016/j.materresbull.2018.11.030.

Scholtzová, E.; Madejová, J.; Tunega, D. 2014. Structural properties of montmorillonite intercalated with tetraalkylammonium cations-Computational and experimental study. Vibrational Spectroscopy 74: 120-126. doi: 10.1016/j.vibspec.2014.07.010.

Schultz, L.G. 1969. Lithium and potassium absorption, dehydroxylation temperature, and structural water content of aluminous smectites. Clays and Clay Minerals 17 (3): 115-149. doi: 10.1346/CCMN.1969.0170302.

Suseno, S.H.; Nurjanah, A.M.; Jacoeb, S.F.; Saraswat, A.M. 2014. Purification of Sardinella sp., Oil: Centrifugation and Bentonite Adsorbent. Advance Journal of Food Science and Technology 6 (1): 60-67. doi: 10.19026/ajfst.6.3031.

Tadros, T.F. 1980. Physical stability of suspension concentrates. Advances in Colloid and Interface Science 12 (2-3): 141-261. doi: 10.1016/0001-8686(80)85006-8.

Thissen, P. 2020. Exchange reactions at mineral interfaces. Langmuir 36 (35): 10293-10306. doi: 10.1021/acs.langmuir.0c01565.

Tyagi, B.; Chudasama, C.D.; Jasra, R.V. 2006. Determination of structural modification in acid activated montmorillonite clay by FT-IR spectroscopy. Spectrochimica Acta Part A: Molecular and Biomolecular Spectroscopy 64 (2): 273-278. doi: 10.1016/j.saa.2005.07.018.

Unger, K.K. 1979. Porous silica its properties and use as support in column liquid chromatography. Journal of Chromatography Library 16: 57-46. doi: 10.1016/S0301-4770(08)60807-6.

Usman, M.A.; Oribayo, O.; Adebayo, A.A. 2013. Bleaching of palm oil by activated local bentonite and kaolin clay from Afashio, Edo-Nigeria. Chemical and Process Engineering Research 10 (2008): 1-12.

Wazamtu, I.; Abdullahi Sani, N.; Abdulsalam, A.K.; Abubakar Abdullahi, U. 2013. Extraction and quantification of silicon from silica sand obtained from Zauma River, Zamfara State, Nigeria. European Scientific Journal 9 (15): 160-168.

Wilson, M.J. 1994. Clay Mineralogy: Spectroscopic and Chemical Determinative Methods. Chapman and Hall: 367 p. London .doi: 10.1007/978-94-011-0727-3.

Zhang, Y.; Shao, D.; Yan, J.; Jia, X.; Li, Y.; Yu, P.; Zhang, T. 2016. The pore size distribution and its relationship with shale gas capacity in organic-rich mudstone of Wufeng-Longmaxi Formations, Sichuan Basin, China. Journal of Natural Gas Geoscience 1 (3): 213-220. doi: 10.1016/j.jnggs.2016.08.002.

Zheng, R.; Gao, H.; Ren, Z.; Cen, D.; Chen, Z. 2017. Preparation of activated bentonite and its adsorption behavior on oil-soluble green pigment. Physicochemical Problems of Mineral Processing 53 (2): 829-845. doi: 10.5277/ppmp170213.

Zhou, X.; Liu, D.; Bu, H.; Deng, L.; Liu, H.; Yuan, P.; Du, P.; Song, H. 2018. XRD-based quantitative analysis of clay minerals using reference intensity ratios, mineral intensity factors, Rietveld, and full pattern summation methods: A critical review. *S*olid Earth Sciences 3 (1): 16-29. doi: 10.1016/j.sesci.2017.12.002.

Manuscript received: July 29, 2020; revised/accepted: January 19, 2021; available online: May 31, 2021.